Processing and Application of Ceramics 13 [2] (2019) 139–148
https://doi.org/10.2298/PAC1902139D

Preparation of carbonate apatite scaffolds using different carbonate solution and soaking time

Fadilah Darus, Mariatti Jaafar*, Nurazreena Ahmad

Biomaterials Niche Area Group, School of Materials and Mineral Resources Engineering, Engineering Campus, Universiti Sains Malaysia, 14300, Nibong Tebal, Pulau Pinang, Malaysia

Received 13 September 2018; Received in revised form 15 February 2019; Accepted 2 May 2019

Abstract

The aim of this study is to fabricate CO_3Ap scaffolds using a dissolution-precipitation reaction during hydrothermal treatment. Beta-tricalcium phosphate (β-TCP) was used as a precursor instead of the commonly used alpha-tricalcium phosphate (α-TCP). Here, the CO_3Ap scaffold fabrication was accomplished in two steps: i) fabrication of β-TCP scaffold using a combination of direct foaming and a sacrificial template and ii) hydrothermal conversion of the β-TCP scaffold at 200 °C in 2 mol/l $NaHCO_3$ and Na_2CO_3 aqueous solutions for 2–10 days. The effect of two different solutions was identified in the dissolution-precipitation reaction. CO_3Ap scaffold with 8.95 wt.% carbonate content was successfully fabricated using a $NaHCO_3$ solution. The average pore size of the scaffold was approximately 180 μm with 72% porosity. The average compressive strength of the CO_3Ap scaffold was 0.7 MPa. Based on the compressive strength and carbonate content results, $NaHCO_3$ aqueous solutions were chosen as carbonate sources for phase transformation to fabricate a CO_3Ap scaffold over 6 days.

Keywords: *apatite, porous materials, bioactivity, hydrothermal treatment, bioceramics*

I. Introduction

Bioactive materials like carbonate apatite, (CO_3Ap) are expected to be ideal bone replacements because they show excellent osteoconductivity and cell-mediated resorbability in bone defects [1]. The dominant inorganic component of bone is CO_3Ap that contains 4–8 wt.% carbonate in an apatitic structure [2–4]. The presence of carbonate in the apatite lattice contributes to the ease of resorption in bony tissue [5]. It means that CO_3Ap is better in biological response as a bone substitute material. However, artificial CO_3Ap bone substitute has not yet been commercialized due to the low thermal stability of carbonate at high-temperature, i.e. CO_3Ap decomposes at 400 °C and pronounced thermal decomposition occurs at 600–700 °C [3]. An alternative method was proposed to fabricate CO_3Ap scaffolds using a dissolution-precipitation reaction during hydrothermal treatment [4,6–9]. Apart from hydrothermal treatment, other methods such as carbonation [10], phosphorization [2] and hydrolysis [11] were able to fabricate CO_3Ap.

* Corresponding authors: tel: +604 599 5262,
e-mail: *mariatti@usm.my*

The hydrothermal treatment in production of CO_3Ap scaffolds was applied for the first time in 2007. The precursors used in previous works are varied; for example, calcite ($CaCO_3$) [2], gypsum [3], calcium hydrogen phosphate dehydrate (DCPA) [9] and alpha-tricalcium phosphate (α-TCP) [1,8,12]. The selection of the precursors is based on their chemical and physical properties. The precursor should have at least one component of CO_3Ap, such as calcium, phosphate or carbonate group [9]. Table 1 summarizes the precursors used by previous researchers to fabricate a CO_3Ap scaffold by hydrothermal treatment [1–3,8,9,12]. α-TCP powder has commonly been used as a precursor to fabricate CO_3Ap scaffolds due to its high solubility, as reported by Tsuru *et al.* [13]. The high solubility of α-TCP in an aqueous carbonate solution will accelerate the formation of nuclei sites and quickly transform to CO_3Ap. Wakae *et al.* [8] also used α-TCP foam as a precursor in their research study. α-TCP foam was immersed in 4 mol/l sodium carbonate (Na_2CO_3) at 100 and 200 °C for various periods up to 72 h. Plate-like crystals obtained after treatment at 200 °C had a smooth surface whereas the crystals obtained after the treat-

Table 1. Types of precursor used in the fabrication of CO_3Ap scaffold by hydrothermal treatment

Precursors	Carbonate source	Parameters	Amount of carbonate apatite	Year and reference
Calcium hydrogen phosphate dehydrate (DCPA)	$NaHCO_3$ Na_2CO_3	τ_s = 3, 7, 14 days	- 12.9 wt.% - 15.8 wt.%	2017 [9]
α-TCP foam	$NaHCO_3$	C_s = 0.1, 0.2, 0.5 mol/l	0.55–0.85 wt.%	2016 [1]
Gypsum	Na_2HPO_4 $NaHCO_3$	T = 80, 100, 120 °C τ_s = 6, 12, 24, 48, 72 h	1.96–7.18 wt.%	2014 [3]
α-TCP scaffold and β-TCP scaffold	Na_2CO_3 solution	τ_s = 4, 7, 10 days	No data reported	2014 [13]
Gypsum-calcite composite	$(NH_4)_3PO_4$	C_p = 20, 40, 60, 80, 90 wt.% of calcite	0.17–8.55 wt.%	2008 [2]
α-TCP foam	$(NH_4)_2CO_3$	C_s = 0.25, 0.50, 1.00, 2.00, 4.00, 6.00 mol/l	max of 7.4 wt.%	2007 [8]

τ_s - soaking time, C_s - concentrations of solution, C_p - concentrations of solution

ment at 100 °C were constructed from spherical particles. Based on these results, it was concluded that the crystal morphology of the surface is governed by the hydrothermal treatment temperature.

Wakae *et al.* in their work [14] investigated the effect of different concentrations of ammonium carbonate $(NH_4)_2CO_3$ solution on the formation of CO_3Ap at 200 °C for 24 h. After treatment in different concentration solutions, crystals of different morphology were observed. Sugiura *et al.* [1] investigated the setting reaction of α-TCP foam granules in the carbonate salt solution. Different concentrations of sodium hydrogen carbonate ($NaHCO_3$) solution were used in this treatment. Treatment with higher $NaHCO_3$ concentration solutions results in increased CO_3 content in the apatitic structure and the morphology changes from fibre-like to plate-like with a small aspect ratio. The surface characteristics are also governed by the type and concentration of the used solution. When treated with Na_2CO_3 and $NaHCO_3$, the crystal morphology changes to plate-like crystals. In contrast, the crystal structure changed to needle-like when immersed in $(NH_4)_2CO_3$.

Motivated by the research in transforming a precursor to carbonate apatite scaffold, this study is carried out to fabricate CO_3Ap scaffolds using beta-tricalcium phosphate (β-TCP; $Ca_3(PO_4)_2$) as a precursor and compare the effects of two different carbonate solutions used in the phase transformation. To the best of our knowledge, only limited study has been done on β-TCP scaffolds as a precursor due to its lower solubility [13]. This means that a longer transformation time is required to obtain single phase apatite structure. However, β-TCP showed some advantages, for example it exhibits higher mechanical strength compared to α-TCP, as reported by Ahmad *et al.* [15]. Apart from that, the cost of β-TCP powder is much lower than α-TCP powder. Tsuru *et al.* [13] demonstrated the possibility of using β-TCP as a precursor for CO_3Ap scaffold fabrication even though its solubility is much lower compared to other precursors, like α-TCP. However, there is no data reported by Tsuru *et al.* [13] on the carbonate content of these scaffolds after transforming the phase. Pieters *et al.* [11] claimed that carbonate content equal to or greater than 6.9 wt.% is optimal for the formation of appropriate adsorbed surface layer in terms of cell adhesion. Hence, the aim of this study is to investigate the use of β-TCP scaffold (from β-TCP powder) as a precursor to produce CO_3Ap scaffolds. The time required for the transformation of β-TCP to CO_3Ap scaffold was identified. Additionally, the effect of soaking time on the hydrothermal treatment of the β-TCP scaffold in different carbonate solutions was investigated.

II. Experimental

2.1. Materials

The raw material used for scaffold fabrication was β-tricalcium phosphate (β-TCP, $Ca_3(PO_4)_2$), supplied by Sigma-Aldrich Corporation with a molecular weight of 310.18 g/mol. Polyvinyl alcohol (PVA) was purchased from Sigma-Aldrich Corporation in the form of powder with a specified molecular weight average of 72000. PVA was used as a binder. Poly-methyl-methacrylate (PMMA) was purchased from the Chi Mei Company. PMMA pellets size was in the range of 50–150 μm and it was used as a pore former for the sacrificial template. Hydrogen peroxide (H_2O_2) was purchased from J.T. Baker® Chemicals in liquid form. H_2O_2 was used as a foaming agent for direct foaming techniques. For the phase transformation reaction, sodium hydrogen carbonate ($NaHCO_3$) and sodium carbonate (Na_2CO_3) were used. $NaHCO_3$ and Na_2CO_3 with a molar mass of 84.01 g/mol and 105.99 g/mol, respectively, were supplied by Merck Germany. These two materials were used as a carbonate source in hydrothermal treatment.

2.2. Fabrication of β-TCP and CO_3Ap scaffolds

β-TCP scaffolds were fabricated using a combined method consisting of direct foaming and a sacrificial template. This method was modified from previous work by Zairani *et al.* [16]. β-TCP powder (95 wt.%) was mixed with 5 wt.% PMMA pellets and H_2O_2 solu-

tion at a liquid to powder ratio (L/P ratio) of 0.38 ml/g. About 4 wt.% PVA binder was added into the mixture and homogenized using a mechanical stirrer for half an hour until a homogeneous paste was form. The paste was then transferred into a polypropylene (PP) mould and kept in an oven (Memmert) at 60 °C for 24 h. At this temperature the foaming process occurs, where the decomposition of H_2O_2 produces H_2O and O_2 bubbles. Next, the green sample was removed from the PP mould and heated at 400 °C for 1 h at a heating rate of 1 °C/min to burn out the PMMA. Finally, the sample was sintered in a furnace (Lenton Muffle Furnace 1200) at 1100 °C for 2 h with a ramp rate of 5 °C/min followed by furnace cooling.

The prepared β-TCP scaffold was subjected to hydrothermal treatment with two different carbonate solutions, $NaHCO_3$ and Na_2CO_3. Aqueous solutions of both $NaHCO_3$ and Na_2CO_3 were prepared at 2 mol/l concentration. Then, the β-TCP scaffold was immersed in these solutions in a Teflon vessel with a stainless-steel jacket for the hydrothermal treatment and kept in an oven (Lenton) at 200 °C for 2, 4, 6, 8 and 10 days. After the hydrothermal reaction, the specimens were removed from the vessels, rinsed with distilled water and dried at room temperature for 24 h. Figure 1 shows the schematic diagrams of the fabrication of CO_3Ap scaffolds.

2.3. Characterizations

The morphology of β-TCP scaffold before and after hydrothermal reaction was characterized using field emission scanning electron microscopy (FESEM, Model: Zeiss Supra 55VP, Germany). The scaffolds were mounted on aluminium stubs with double carbon tape and sputtered with a thin gold layer using a Polaron SC 515. The average pore size was measured using 30 readings from the ImageJ software program. X-ray diffraction (XRD) analysis was carried out on a Bruker AXS D8 Advance with counter-monochromatic Cu$K\alpha$ radiation generated at 40 kV and 40 mA and 0.034°/s scanning rate. The samples were scanned in 2θ range 10–90° and with wavelength λ = 1.5406 Å as the X-ray source. Fourier transform infrared (FTIR) spectroscopy (Model: PERKIN Elmer Spectrum) was used to detect the functional groups of the scaffold after hydrothermal treatment. Infrared spectra were measured with a scan parameter range from 4000–400 cm^{-1} using the KBr pellet technique with a spectral resolution of 4 cm^{-1}. The porosity of the scaffolds was measured using a helium pycnometer (AccuPyc II 1340, Micromeritics).

Carbon hydrogen nitrogen (CHN) analysis was used to determine the carbonate content of the scaffold after hydrothermal treatment. A Perkin Elmer Series 2, 2400 CHNS/O elemental analyser was used to measure the CO_3^{2-} content. The Ca/P molar ratio of the scaffold after the hydrothermal treatment in $NaHCO_3$ and Na_2CO_3 aqueous solutions was determined by EDAX, Genesis. The compressive strength of the scaffolds was measured using an Instron 3369 according to ASTM-D-695-96 at a crosshead speed of 1.0 mm/min and 5 kN cell load. Eight samples were used for the measurement of each parameter.

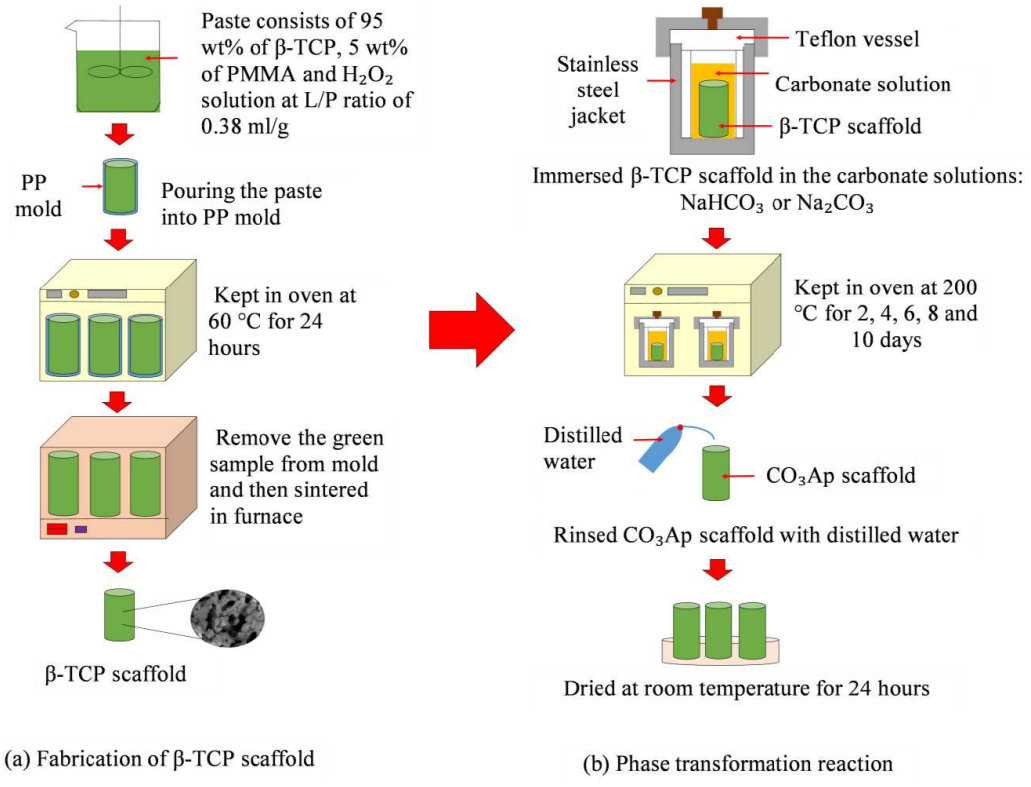

Figure 1. Schematic diagrams of: a) fabrication of β-TCP scaffold and b) phase transformation reaction

III. Results and discussion

Structure and morphology of the β-TCP scaffold fabricated by the combined method consisting of direct foaming and sacrificial template are shown in Fig. 2. In this method, PMMA was used as a pore former for the sacrificial template while H_2O_2 acts as a foaming agent. From Figs. 2b and 2c, the β-TCP scaffold consists of an interconnected network of pores with a coral-reef-like structure. This is in agreement with the previous work reported by Zairani *et al.* [16], who used the same method to fabricate the scaffold. The interconnected network that links one pore to another is a result of the presence of H_2O_2 which acts as a former agent during the foaming process. In the foaming process, the decomposition of H_2O_2 formed H_2O and O_2 and produced bubbles. The porosity of the fabricated β-TCP scaffold was around 74%.

The interconnected pores consisted of micropores, mesopores and macropores. According to the International Union of Pure and Applied Chemistry (IUPAC) classification of pore size, the micropore width does not exceed 2 nm, the mesopore width is in the 2–50 nm range and the macropore width is above 50 nm [17,18]. These pores' function is to transfer nutrients and oxygen in tissue engineering [19]. Based on 30 measurements, the average pore sizes of the β-TCP scaffold are 184 μm for larger macropores and 1.80 μm for smaller macropores. Figure 3 shows the distribution graph of larger and smaller macropores. From the graph, the most frequent values of the larger macropores are found in the middle of the 150–200 μm distribution range and the curve shape taper off from the middle in a normal distribution. The larger macropores are normally distributed with a mean value of 184 μm. For the smaller macropores, the distribution is not even close to forming a normal curve. However, the most frequent value remains around the middle of a bell curve with a mean of 1.80 μm. Overall, both distributions, either for the larger or smaller macropores, are still evenly distributed at the centre, with the mean capturing 95.44% of the area under the curve.

Before the hydrothermal treatment reaction, the smooth surface of the β-TCP scaffold was observed as shown in Figure 2. However, after hydrothermal treatment, the microstructure of the scaffold changed depending on the type of immersion solution used. During hydrothermal treatment, the dissolution and precipitation reactions occur. Dissolution of the β-TCP scaffold achieved a balance and continuous dissolution in order to release both Ca^{2+} and PO_4^{3-} ions into the solution, as shown in Eq. 1. When the β-TCP scaffold was soaked in the solution containing CO_3^{2-} ions, the solution is supersaturated with respect to carbonate apatite. Thus, Ca^{2+}, PO_4^{3-} and CO_3^{2-} were precipitated on the surface of the β-TCP scaffold as carbonate apatite (Eq. 2) as reported by Kunio *et al.* [20]. Carbonate apatite crystals were precipitated and entangled to each other.

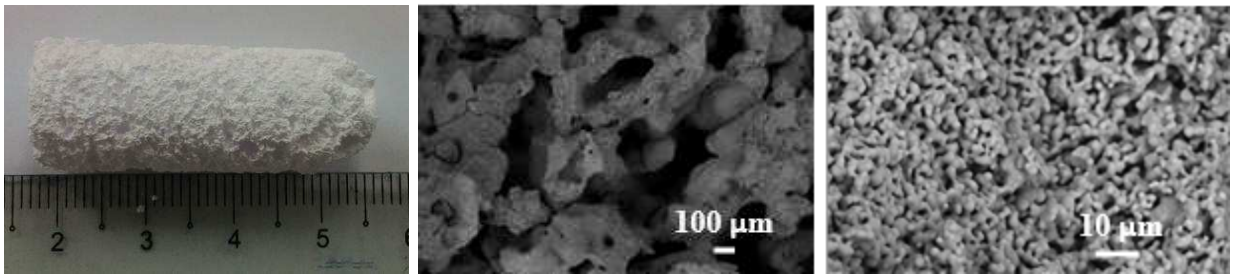

(a) (b) (c)

Figure 2. β-TCP scaffold fabricated by a combination method of direct foaming and sacrificial template: a) photography and SEM micrographics at magnification of b) 60× and c) 1000×

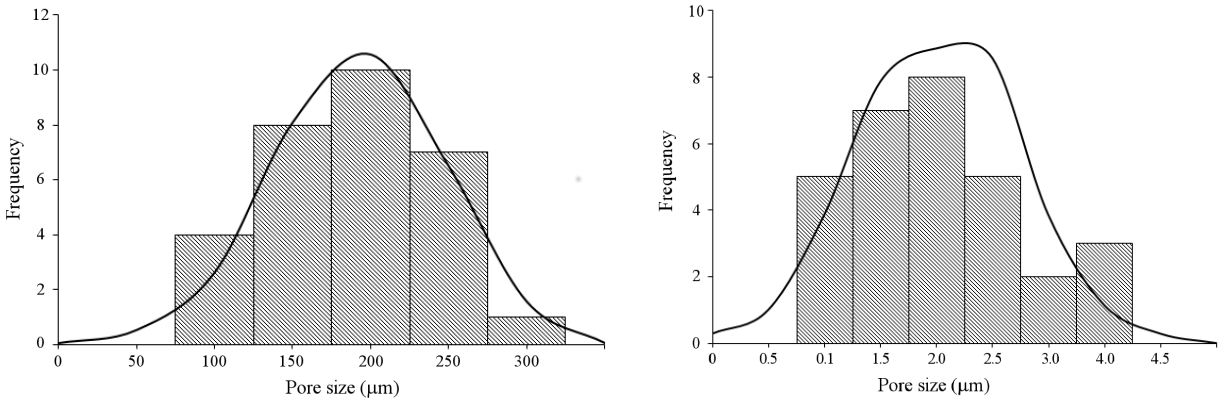

(a) (b)

Figure 3. Distribution graph of: a) larger and b) smaller macropores

$$Ca_3(PO_4)_2 \longrightarrow 3\,Ca^{2+} + 2\,PO_4^{3-} \quad (1)$$

$$Ca^{2+} + PO_4^{3-} + CO_3^{2-} \longrightarrow Ca_{10-a}(PO_4)_{6-b}(CO_3)_c(OH)_{2-d} \quad (2)$$

Figures 4 and 5 show SEM images of β-TCP scaffolding after hydrothermal treatment with 2 mol/l $NaHCO_3$ and Na_2CO_3 aqueous solution, respectively, at 200 °C for 2, 4, 6, 8 and 10 days. All scaffolds maintained their interconnected pores after treatment with either $NaHCO_3$ or Na_2CO_3 aqueous solutions. This is in agreement with previous works reported by Sugiura *et al.* [1] in their study on the setting reaction of α-TCP foam granules. However, the microstructure differed after treatment in both carbonate solutions. After 2 days treatment in both carbonate solutions, small crystals (in a circle) were found on the surface of the scaffold at higher magnification. However, based on a comparison in terms of crystal formation on the scaffold, the formation of crystals is faster in $NaHCO_3$ than Na_2CO_3 aqueous solution. This is due to the difference in pH values of the carbonate solution used in the treatment. In a dissolution-precipitation reaction, precipitation cannot occur without prior dissolution of the starting materials. The dissolution of starting materials is accelerated in acidic conditions, as mentioned by Cahyanto *et al.* [21]. In other words, the dissolution of materials was slower in an alkaline solution. $NaHCO_3$ and Na_2CO_3 aqueous solutions pH measurements indicate that $NaHCO_3$ is less alkaline, with a pH of 10.50, than Na_2CO_3, with a pH of 11.64. That is why precipitation of CO_3Ap crystals occurs faster when treated in $NaHCO_3$ aqueous so-

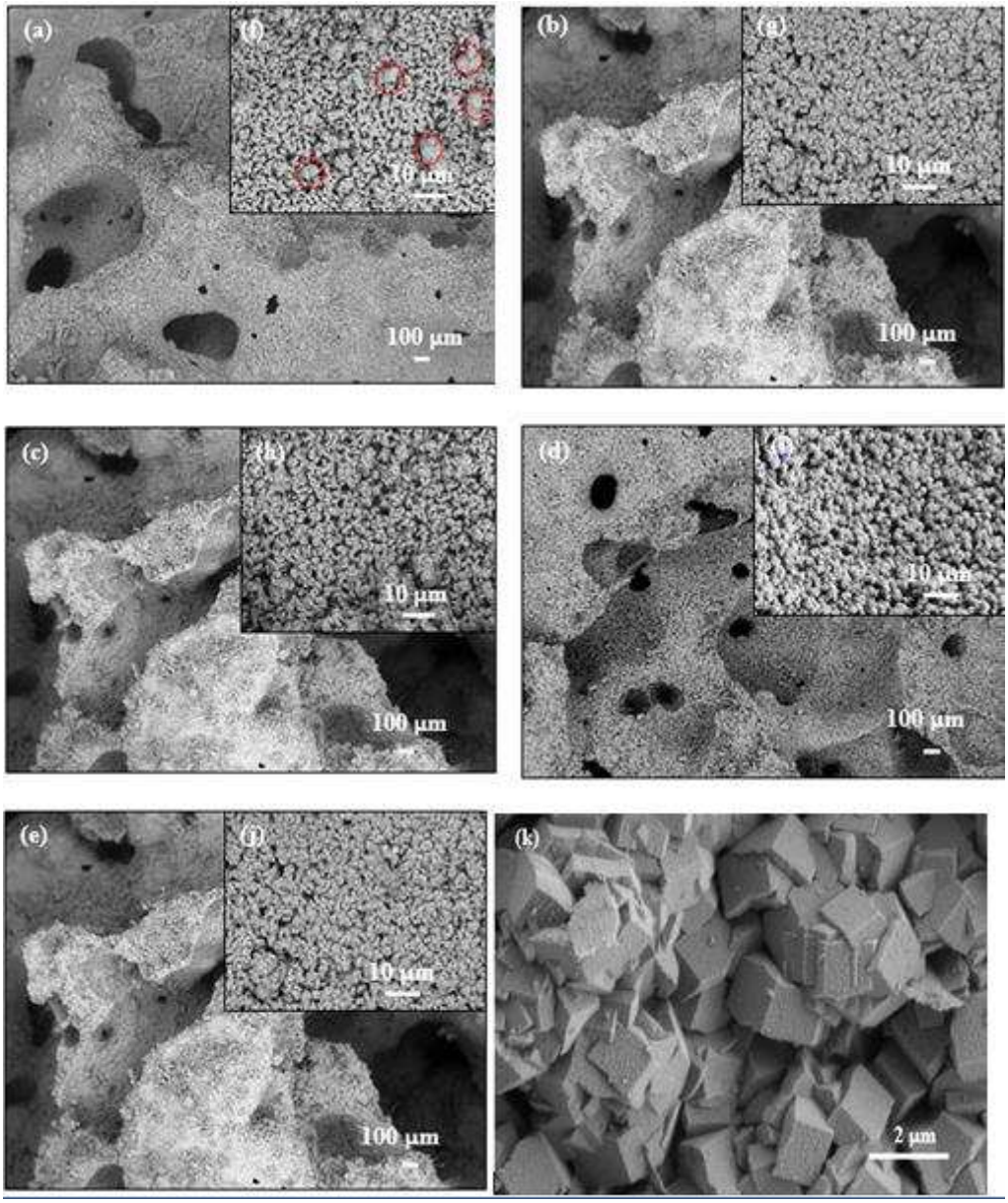

Figure 4. Morphology of β-TCP scaffold after hydrothermal treatment with 2 mol/l $NaHCO_3$ solution at 200 °C for various soaking time: a) 2, b) 4, c) 6, d) 8, e) 10 days (SEM images with higher magnifications are given in insets) and k) 6 days observed at magnification of 5000×

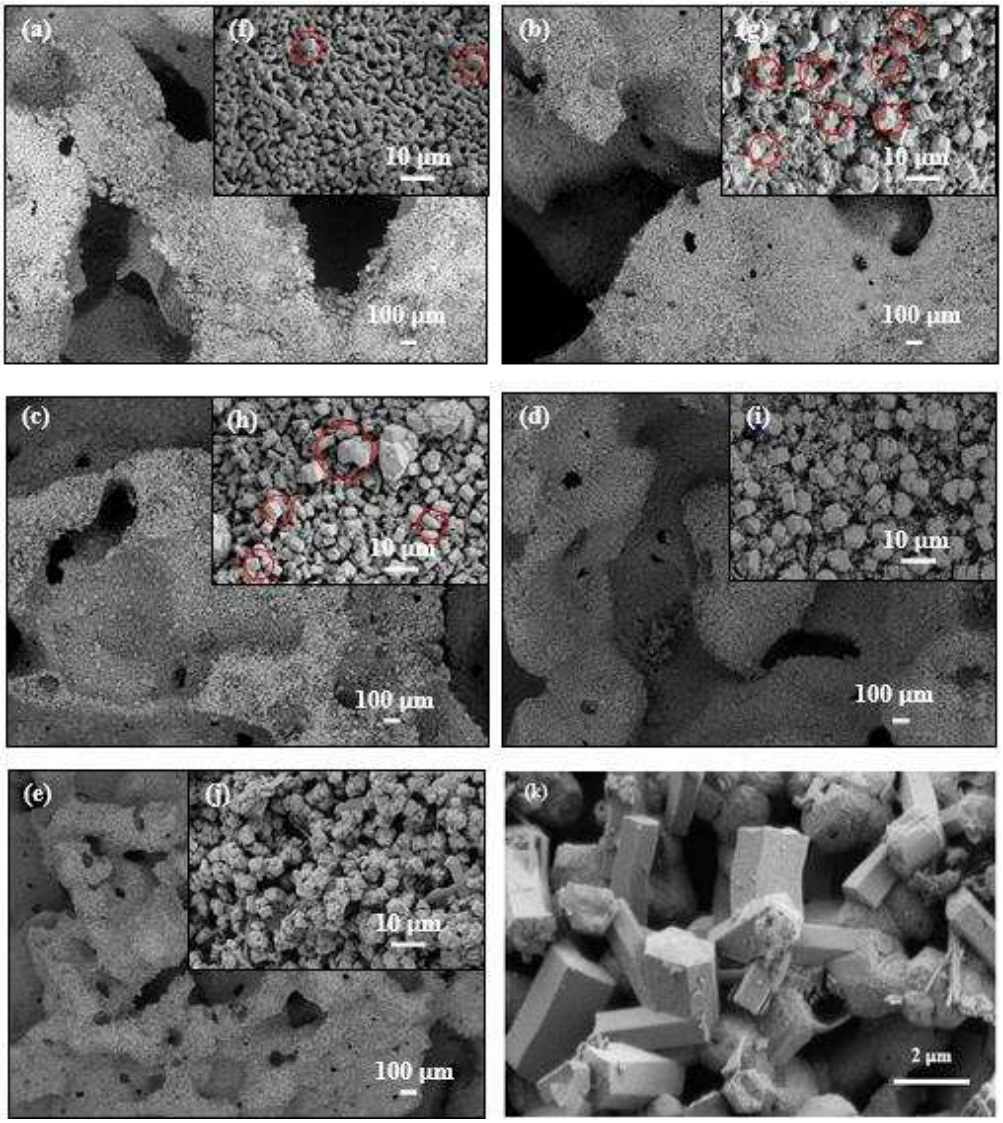

Figure 5. Morphology of β-TCP scaffold after hydrothermal treatment with 2 mol/l Na_2CO_3 solution at 200 °C for various soaking time: a) 2, b) 4, c) 6, d) 8, e) 10 days (SEM images with higher magnifications are given in insets) and k) 6 days observed at magnification of 5000×

lution compared to Na_2CO_3 aqueous solution after 2 days of treatment. As the dissolution of β-TCP scaffolding is higher in a $NaHCO_3$ solution, the concentration of Ca^{2+} and CO_3^{2-} ions quickly increased and it easily reached supersaturation with respect to apatite, as shown in Eq. 2.

Prolonging the soaking time from 4 to 10 days in both carbonate solutions, caused a lot of small crystals to appear on the surface. This is due to the precipitated apatite crystals interlocking with each other to set and form larger apatite crystals. A similar observation was reported by Sugiura *et al.* [1] and Ishikawa *et al.* [7], where a lot of small crystals appeared on the α-TCP foam after treatment with $NaHCO_3$ and saturated sodium bicarbonate, respectively. The surface structure of the crystals was clearly revealed at higher magnification (insets in Fig. 4). However, the polygon-like crystals observed were larger in size when treated in Na_2CO_3 aqueous solution. This is due to the slow solubility of β-TCP scaffolding in Na_2CO_3. In contrast, when treated with $NaHCO_3$ solution, the crystals were closely attached and aligned with each other to form crystal entanglements, as reported by Trusu *et al.* [13], due to high supersaturation with respect to apatite. There is not much observed difference in the crystal morphology of scaffold after hydrothermal treatment regardless of using $NaHCO_3$ or Na_2CO_3 aqueous solution. The crystals maintain the polygon-like shape [1,10,11]. This result is in agreement with Tsuru *et al.* [9], where it was reported that polygon-like crystals were formed on the DCPA scaffold when immersed in 2 mol/l of Na_2CO_3 aqueous solution.

Figures 6 and 7 show the XRD patterns of β-TCP scaffold before and after hydrothermal treatment in the presence of 2 mol/l $NaHCO_3$ and Na_2CO_3 aqueous solution at 200 °C for 2, 4, 6, 8 and 10 days, respectively. The pattern of commercial hydroxyapatite (HAp) is also shown in both graphs as a reference due to the similarity

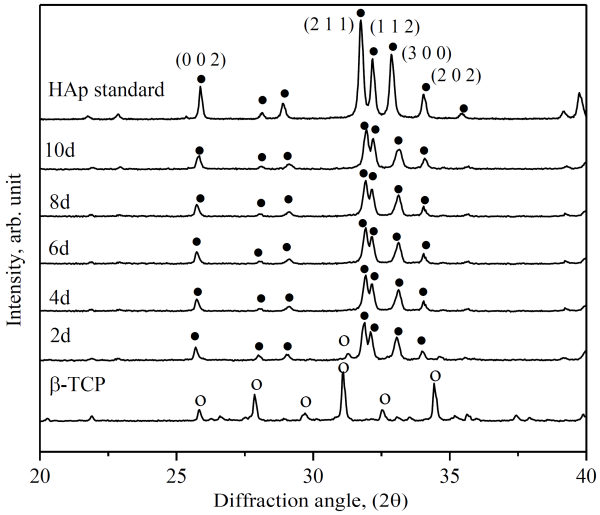

Figure 6. XRD pattern of β-TCP scaffold before and after hydrothermal reaction with 2 mol/l $NaHCO_3$ at 200 °C with various soaking time

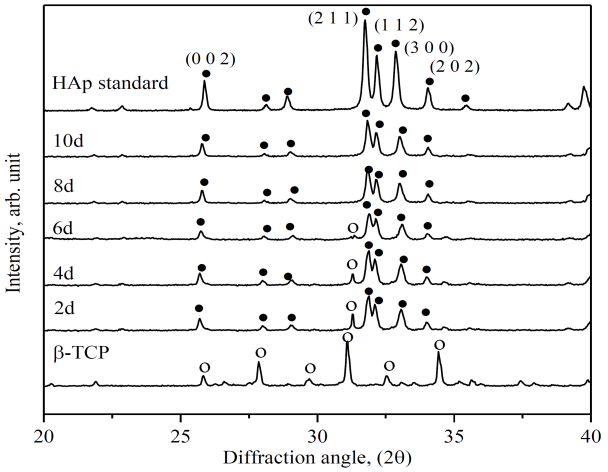

Figure 7. XRD pattern of β-TCP scaffold before and after hydrothermal reaction with 2 mol/l Na_2CO_3 at 200 °C with various soaking time

in the crystal structure with apatite [22]. No other phase was detected before treatment, indicating that the starting materials were β-TCP scaffold. After treatment in both carbonate solutions, β-TCP scaffold transforms to CO_3Ap to varying extent by soaking time. After 2 days treatment in $NaHCO_3$ (Figure 6), most of the peaks assigned to β-TCP disappeared and peaks assigned to apatite at (002), (211), (112), (300) and (202), as reported by Pieters *et al.* [11], were detected. The same trend, where peaks corresponding to apatite appeared, was observed when prolonging the soaking time to 10 days.

After immersion in Na_2CO_3 (Fig. 7), peaks assigned to β-TCP were observed for 2, 4 and 6 days, whereas they disappeared completely after 8 days of treatment. In other words, the longer period in Na_2CO_3 caused complete conversion of β-TCP into apatite, using either $NaHCO_3$ or Na_2CO_3 aqueous solution during hydrothermal treatment.

Figure 8 shows the comparison of the conversion rate from β-TCP scaffold to CO_3Ap after hydrothermal treatment in the presence of 2 mol/l $NaHCO_3$ and Na_2CO_3 aqueous solution at 200 °C for 2, 4, 6, 8 and 10 days. The conversation rate to apatite was calculated from the quantitative phase composition using Rietveld refinement from X-pert Highscore Plus software. According to the graph (Fig. 8), the conversion to apatite is faster with treatment in $NaHCO_3$ solution compared to treatment in Na_2CO_3 solution for 2 days treatment. The conversion to apatite was 100% completed when treated in $NaHCO_3$ solution for 6 days. While for Na_2CO_3 solution, the conversion was almost complete, 95%, within 6 days. When prolonging the soaking time from 8 to 10 days in both solutions, the conversion to apatite was 100%. Therefore, in conclusion, the conversion of β-TCP to CO_3Ap scaffold is faster in $NaHCO_3$ aqueous solution.

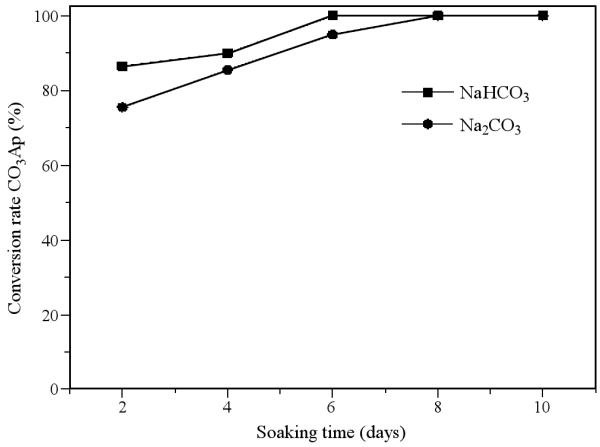

Figure 8. Conversion rates to CO_3Ap as a function of time with different carbonate solutions

FTIR spectra of β-TCP scaffold before and after hydrothermal treatment in the presence of 2 mol/l $NaHCO_3$ and Na_2CO_3 aqueous solution at 200 °C for 2, 4, 6, 8 and 10 days are shown in Figs. 9 and 10, respectively. β-TCP scaffold shows absorption bands at 605 cm^{-1} in the wavenumber region of 610–554 cm^{-1}, which is assigned to P–O vibration modes of the PO_4^{3-} group in β-TCP. This result is in agreement with the previous report on the wave region of P–O vibration modes by Mirhadi *et al.* [23]. Absorption band at 3436–3468 cm^{-1} is assigned to adsorbed water in the β-TCP scaffold [24]. After hydrothermal treatment in both carbonate aqueous solutions for 2–10 days, the absorption band assigned to P–O and C–O in PO_4^{3-} and CO_3^{2-} were detected at vibration modes of 604 cm^{-1} and 1350–1550 cm^{-1} and 870 cm^{-1}, respectively. The absorption band of CO_3^{2-} in these spectra belong to the CO_3^{2-} group in B-type CO_3Ap in which PO_4^{3-} is partially substituted by CO_3^{2-}. These bands were correlated with CO_3^{2-} of the typical B-type CO_3Ap, as reported in previous works [4,14,17,23–25]. This result indicates that transformation to CO_3Ap was completed using either $NaHCO_3$ or Na_2CO_3 aqueous solution as the carbonate

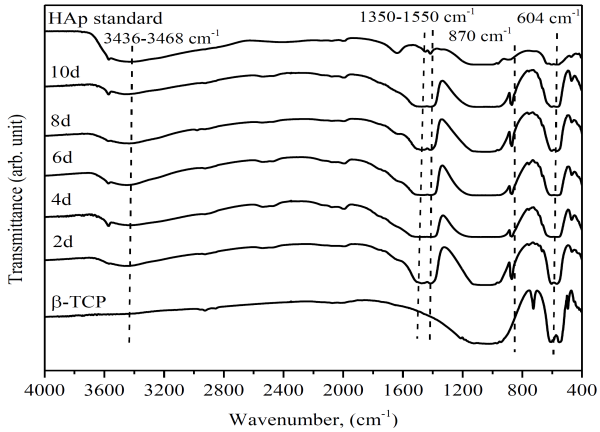

Figure 9. FTIR spectra of β-TCP scaffold before and after hydrothermal reaction with 2 mol/l $NaHCO_3$ at 200 °C with various soaking time

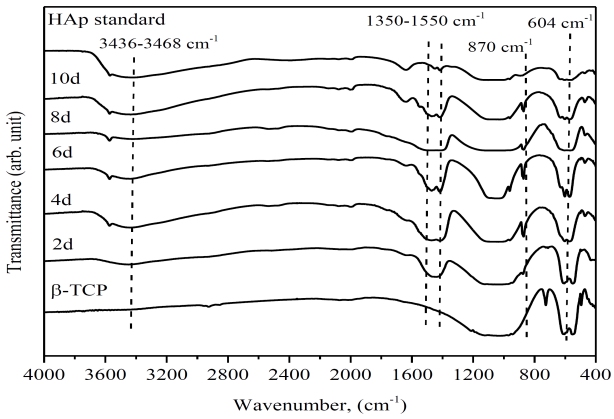

Figure 10. FTIR spectra of the β-TCP scaffold before and after hydrothermal reaction with 2 mol/l Na_2CO_3 at 200 °C with various soaking time

supply source. The conversion to apatite was supported by the XRD results (Figs. 6 and 7), where the peak assigned to apatite was present.

The Ca and P content and the molar Ca/P ratio of the β-TCP scaffold after hydrothermal treatment are summarized in Table 2. These values were compared to the stoichiometric ratio of β-TCP (Ca/P = 1.31) as a starting material. When treated in both carbonate solutions, either $NaHCO_3$ or Na_2CO_3, the Ca/P ratio increases. This is due to the substitution of PO_4^{3-} ions with CO_3^{2-} during the dissolution-precipitation reaction as reported by Pieters *et al.* [11]. As the Ca content increases, the P content decreases. The range for the Ca/P molar ratio of CO_3Ap was reported as 1.7–2.6; thus, the Ca/P ratios from 1.71–2.23 in this study agreed well with the previous reports by LeGeros [26] and Bang *et al.* [27].

The carbonate contents of the CO_3Ap scaffolds calculated from the CHN analysis are summarized in Fig. 11. The carbonate content was observed in the range of 2–11%. The carbonate content increased with increasing hydrothermal treatment soaking time for both carbonate solutions used. However, the carbonate content of β-TCP scaffold immersed in $NaHCO_3$ aqueous solution is higher than that from immersion in Na_2CO_3 aqueous solution. This is because of the substitution of PO_4^{3-} by CO_3^{2-} during the dissolution-precipitation reaction. Pieters *et al.* [11] claimed that carbonate content equal to or greater than 6.9 wt.% is an optimum composition and structure of the adsorbed surface layer in terms of cell adhesion. Theoretically, high carbonate

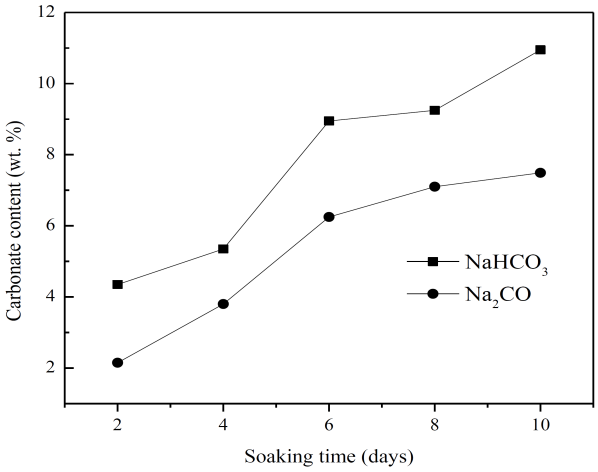

Figure 11. Carbonate content in CO_3Ap obtained by hydrothermal treatment of β-TCP scaffold in $NaHCO_3$ and Na_2CO_3 aqueous solutions

Table 2. Ca, P and molar Ca/P ratio of β-TCP scaffold after hydrothermal treatment in $NaHCO_3$ and Na_2CO_3 aqueous solutions

Sample	Treatment time [day]	Contents [wt.%]		Molar Ca/P ratio
		Ca	P	
β-TCP scaffold	-	36.38	21.46	1.31
β-TCP scaffold treated in $NaHCO_3$	2	42.19	24.32	1.34
	4	42.29	20.37	1.61
	6	43.98	19.80	1.71
	8	44.86	18.04	1.92
	10	52.49	18.22	2.23
β-TCP scaffold treated in Na_2CO_3	2	33.26	18.43	1.39
	4	39.82	20.77	1.48
	6	44.09	22.23	1.53
	8	47.07	21.07	1.73
	10	48.30	19.91	1.87

content could be advantageous for bone-related applications, by allowing optimum adsorption of proteins and improving cell adhesion. Higher carbonate contents are also associated with less crystalline and more soluble apatite [28]. Additionally, carbonate contents equal to or higher than 11% are reported able to support high cell proliferation [11].

Based on the SEM observations, there is not much difference in the average larger macropore size of the scaffolds after hydrothermal treatment, either in $NaHCO_3$ or Na_2CO_3 aqueous solution. Smaller macropores of scaffold cannot be measured due to the surface being covered with apatite crystals after the treatment in either carbonate solution. The porosity of the scaffold after treatment also shows insignificant difference. The porosity of the β-TCP scaffold before hydrothermal treatment is 74% and decreases to 72% and 69% after treatment in $NaHCO_3$ or Na_2CO_3 solutions, respectively. The percentage of porosity is still significant enough to be used in tissue engineering applications where the required porosity is within the 50–90% range. Wakae *et al.* [8] also reported similar results, where the pore size and porosity of the α-TCP foam remained unchanged before and after hydrothermal treatment in $(NH_4)_2CO_3$ solution.

Figure 12 summarizes the compressive strength of the β-TCP scaffold before and after immersion in both carbonate solutions. The strength of the β-TCP scaffold before and after the hydrothermal treatment shows a slight increasing trend with increasing soaking time. The compressive strength of the β-TCP/$NaHCO_3$ was slightly higher compared to β-TCP/Na_2CO_3. This is due to the difference in the crystal structure of β-TCP scaffold after the treatment in both solutions. The crystal transformation of the β-TCP scaffold after treatment in $NaHCO_3$ aqueous solution was accelerated, resulting in interlocking between crystals, as shown in Fig. 2k. Cahyanto *et al.* [21] reported that the crystals will interlock to set and harden. Although slightly different mechanical properties were reported, there were no differences in term of scaffolds' porosity treated in either $NaHCO_3$ or Na_2CO_3 aqueous solution.

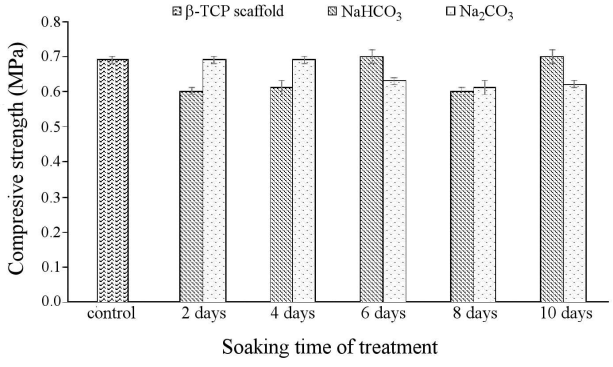

Figure 12. Compressive strengths of the β-TCP scaffolds before and after hydrothermal treatment in $NaHCO_3$ and Na_2CO_3 aqueous solutions

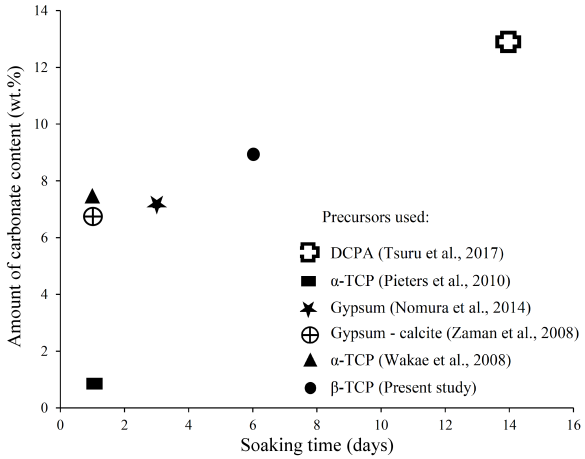

Figure 13. Theoretical and experimental soaking time and amount of carbonate content of scaffolds in previous studies and present work

A correlation between the carbonate content and soaking time of CO_3Ap scaffold reported using different precursors is presented in Fig. 13. Based on the previous works and the results obtained from this study, the soaking time varied from 1–14 days and the carbonate content varied from 0.85–12.9%. In general, the soaking times for scaffolds in these studies were different depending on the precursors, type of solution, concentration and pH of the solution used during hydrothermal treatment. It should be stressed here that most of the previous work used α-TCP [1,8] and gypsum [2,3] as precursors, which will accelerate the transformation of apatite. They also considered DCPA as a starting precursor instead of β-TCP which has been considered in this study. Based on Fig. 13, the results from this study fall in between data reported in the previous works. This study shows that only 6 days are required to transform from β-TCP to CO_3Ap scaffold when the carbonate content is 8.95%. This means that the carbonate content of this research study corresponds well to previous works and β-TCP could be used as a starting material to fabricate CO_3Ap. However, it should be reiterated here that factors such as precursors, solution composition, and pH of the solution might contribute to the degree of supersaturation of the solution with respect to CO_3Ap.

IV. Conclusions

CO_3Ap scaffold was successfully prepared using β-TCP as a precursor through a dissolution-precipitation reaction in the presence of $NaHCO_3$ or Na_2CO_3 aqueous solution. The transformation rate from β-TCP to CO_3Ap scaffold increased when the soaking time was prolonged using either $NaHCO_3$ or Na_2CO_3. However, the crystal transformation to apatite was faster in the case of $NaHCO_3$ immersion compared to Na_2CO_3 due to the faster dissolution of starting materials in more acidic conditions. β-TCP scaffold was fully transformed to CO_3Ap after 6 days treatment in $NaHCO_3$ and after 8 days in Na_2CO_3 aqueous solutions. Based on

the compressive strength and carbonate content results, $NaHCO_3$ aqueous solution was chosen as the carbonate source for phase transformation to fabricate CO_3Ap scaffold over 6 days with a compressive strength of 0.7 MPa.

Acknowledgement: The authors would like to thank Ministry of Education Malaysia for the financial support through Trans Disciplinary Research Grant Scheme (TRGS), grant no 6761004 and the School of Materials and Mineral Resources Engineering for laboratory cooperation.

References

1. Y. Sugiura, K. Tsuru, K. Ishikawa, "Fabrication of carbonate apatite foam based on the setting reaction of α-tricalcium phosphate foam granules", *Ceram. Int.*, **42** (2015) 204–210.
2. C.T. Zaman, A. Takeuchi, S. Matsuya, Q.H.M.S. Zaman, K. Ishikawa, "Fabrication of B-type carbonate apatite blocks by the phosphorization of free-molding gypsum-calcite composite", *Dent. Mater. J.*, **27** (2008) 710–715.
3. S. Nomura, K. Tsuru, M. Maruta, S. Matsuya, I. Takahashi, K. Ishikawa, "Fabrication of carbonate apatite blocks from set gypsum based on dissolution precipitation reaction in phosphate-carbonate mixed solution", *Dent. Mater. J.*, **33** (2014) 166–172.
4. M. Maruta, S. Matsuya, S. Nakamura, K. Ishikawa, "Fabrication of low-crystalline carbonate apatite foam bone replacement based on phase transformation of calcite foam", *Dent. Mater. J.*, **30** (2011) 14–20.
5. Y. Doi, T. Shibutani, Y. Moriwaki, T. Kajimoto, Y. Iwayama, "Sintered carbonated apatites as bioresorbable bone substitutes", *J. Biomed. Mater. Res.*, **39** (1998) 603–610.
6. A. Almirall, G. Larrecq, J.A. Delgado, S. Martínez, J.A. Planell, M.P. Ginebra, "Fabrication of low temperature macroporous hydroxyapatite scaffolds by foaming and hydrolysis of an a-TCP paste", *Biomaterials*, **25** (2004) 3671–3680.
7. K. Ishikawa, K. Udoh, H. Wakae, M.L. Munar, S. Matsuya, M. Nakagawa, A. Nakajima, "Fabrication of carbonate apatite form and its basic properties", *Key Eng. Mater.*, **284-286** (2005) 373–376.
8. H. Wakae, A. Takeuchi, K. Udoh, S. Matsuya, M.L. Munar, R.Z. LeGeros, A. Nakasima, K. Ishikawa, "Fabrication of macroporous carbonate apatite foam by hydrothermal conversion of a-tricalcium phosphate in carbonate solutions", *J. Biomed. Mater. Res. - Part A*, **87** (2007) 957–963.
9. K. Tsuru, A. Yoshimoto, M. Kanazawa, Y. Sugiura, Y. Nakashima, K. Ishikawa, "Fabrication of carbonate apatite block through a dissolution-precipitation reaction using calcium hydrogen phosphate dihydrate block as a precursor", *Materials*, **10** (2017) 374.
10. A. Cahyanto, K. Tsuru, K. Ishikawa, "Transformation of apatite cement to B-type carbonate apatite using different atmosphere", *Key Eng. Mater.*, **696** (2016) 9–13.
11. I.Y. Pieters, N.M.F. Van den Vreken, H.A. Declercq, M.J. Cornelissen, R.M.H. Verbeeck, "Carbonated apatites obtained by the hydrolysis of monetite: Influence of carbonate content on adhesion and proliferation of MC3T3-E1 osteoblastic cells", *Acta Biomater.*, **6** (2010) 1561–1568.
12. I.D. Ana, S. Matsuya, K. Ishikawa, "Engineering of carbonate apatite bone substitute based on composition-transformation of gypsum and calcium hydroxide", *Engineering*, **2** (2010) 344–352.
13. K. Tsuru, T. Nikaido, M.L. Munar, M. Maruta, S. Matsuya, S. Nakamura, I. Kunio, "Synthesis of carbonate apatite foam using β-TCP foams as precursors", *Key Eng. Mater.*, **587** (2013) 52–55.
14. H. Wakae, A. Takeuchi, S. Matsuya, M.L. Munar, M. Nakagawa, K. Udoh, A. Nakashima, K. Ishikawa, "Effects of hydrothermal treatment temperature on the crystallinity of cancellous bone type carbonate apatite foam", *Key Eng. Mater.*, **361-363** (2008) 975–978.
15. N. Ahmad, K. Tsuru, M.L. Munar, M. Maruta, S. Matsuya, K. Ishikawa, "Effect of precursor's solubility on the mechanical property of hydroxyapatite formed by dissolution-precipitation reaction of tricalcium phosphate", *Dent. Mater. J.*, **31** (2012) 995–1000.
16. N.A.S. Zairani, M. Jaafar, N. Ahmad, K. Abdul Razak, "Fabrication and characterization of porous β-tricalcium phosphate scaffolds coated with alginate", *Ceram. Int.*, **42** (2016) 5141–5147.
17. K.S.W. Sing, "Characterization of porous solids: An introductory survey", *Stud. Surf. Sci. Catal.*, **62** (1991) 1–9.
18. B. Zdravkov, J.J. Čermák, J. Janků, V. Kučerová, M. Šefara, "Pore classification in the characterization of porous materials", *Chem. List.*, **102** (2008) 434–438.
19. F. Dehghani, N. Annabi, "Engineering porous scaffolds using gas-based techniques", *Curr. Opin. Biotechnol.*, **22** (2011) 661–666.
20. I. Kunio, "Carbonate apatite bone replacement", *Key Eng. Mater.*, **587** (2013) 17–20.
21. A. Cahyanto, M. Maruta, K. Tsuru, S. Matsuya, K. Ishikawa, "Fabrication of bone cement that fully transforms to carbonate apatite", *Dent. Mater. J.*, **34** (2015) 394–401.
22. L.T. Bang, S. Ramesh, J. Purbolaksono, B.D. Long, H. Chandran, R. Othman, "Development of a bone substitute material based on alpha-tricalcium phosphate scaffold coated with carbonate", *Biomed. Mater.*, **10** (2015) 45011.
23. B. Mirhadi, B. Mehdikhani, N. Askari, "Synthesis of nanosized β-tricalcium phosphate via wet precipitation", *Process. Appl. Ceram.*, **5** (2011) 193–198.
24. A. Wang, D. Liu, H. Yin, H. Wu, Y. Wada, M. Ren, T. Jiang, X. Cheng, Y. Xu, "Size-controlled synthesis of hydroxyapatite nanorods by chemical precipitation in the presence of organic modifiers", *Mater. Sci. Eng. C*, **27** (2007) 865–869.
25. G.C. Celotti, E. Landi, M. Sandri, A. Tampieri, "New method to prepare natural-like carbonate apatite for bone replacement", *Key Eng. Mater.*, **264-268** (2004) 2071–2074.
26. R.Z. LeGeros, J.P. LeGeros, "Calcium phosphate bioceramics: Past, present and future", *Key Eng. Mater.*, **240-242** (2003) 3–10.
27. L.T. Bang, B.D. Long, R. Othman, "Carbonate hydroxyapatite and silicon-substituted carbonate hydroxyapatite: Synthesis, mechanical properties, and solubility evaluations", *Sci. World J.*, **2014** (2014) 969876.
28. R.Z. Legeros, O.R. Trautz, J.P. Legeros, E. Klein, W. Paul Shirra, "Apatite crystallites: Effects of carbonate on morphology", *Science*, **155** [3768] (1967) 1409–1411.